arXiv:cond-mat/9906263v1 [cond-mat.str-el] 17 Jun 1999

The small polaron crossover transition in colossal magnetoresistance (CMR) manganites

Unjong Yu and B. I. Min
Department of Physics, Pohang University of Science and Technology, Pohang 790-784, Korea

(February 1, 2008)

Based on the combined model of the double exchange and the polaron, we have studied the small-to-large polaron crossover transition and explored its effects on the magnetic and transport properties in colossal magnetoresistance (CMR) manganites. We have used the variational Lang-Firsov canonical transformation, and shown that the magnetic and transport properties of both high and low T_C manganites are well described in terms of a single formalism. We have reproduced the rapid resistivity drop below T_C, a realistic CMR ratio, and the *first-order-like* sharp magnetic phase transition, which are observed in low T_C manganites.

75.30.Vn,71.38.+i,71.30.+h

Despite intensive researches on the colossal magnetoresistance (CMR) manganites $R_{1-x}A_xMnO_3$ (R = rare-earth; A = divalent cation), there are many unusual properties that remain to be clarified. The most outstanding feature of these compounds is the close relationship between transport phenomena and the magnetism for $0.2 \lesssim x \lesssim 0.5$, which have been traditionally understood by the double exchange (DE) mechanism [1,2]. However, many recent experiments, especially the giant isotope effect in the magnetic transition temperature (T_C) [3], as well as theoretical works [4] indicate that the electron-phonon interaction plays a crucial role in the physics of the CMR manganites. The small-to-large polaron transition near T_C has been reported by various experimental tools [5–9].

The $R_{0.7}A_{0.3}MnO_3$ CMR compounds have a wide range of T_C from 70 K to 365 K depending on the average radius of R and A cations ($\langle r_A \rangle$) [10]. Interestingly, the low T_C manganites are different from the high T_C manganites in many properties. The low T_C manganites have higher resistivity, much sharper resistivity peaks near T_C, and more enhanced magnetoresistance (MR). They often exhibit hysteresis behaviors in the temperature dependent resistivity [10]. Further, in contrast to the other manganites that experience a metal-insulator (M-I) transition near T_C, the highest T_C manganite $La_{0.7}Sr_{0.3}MnO_3$ is metallic in the whole temperature range.

The magnetic moment measurement for $La_{0.67}(Ba_xCa_{1-x})_{0.33}MnO_3$ with varying x shows that the magnetic transition becomes steeper for low T_C samples, reminiscent of the *first-order-like* phase transition for $x = 0.0$ (T_C=340 K and 265 K for $x = 1.0$ and $x = 0.0$, respectively) [11]. Also the NMR measurement for $Pr_{0.7}Ca_{0.15}Sr_{0.15}MnO_3$ (T_C=180 K) and $Pr_{0.7}Ba_{0.3}MnO_3$ ((T_C=175 K) shows that the hyperfine fields on ^{55}Mn nuclei remain finite up to T_C, indicating the first order magnetic transition [12]. Neutron scattering experiment indicates that the spin dynamics near T_C of low T_C $Nd_{0.7}Sr_{0.3}MnO_3$ (T_C=197.9 K) is very distinct from that of high T_C $Pr_{0.7}Sr_{0.3}MnO_3$ (T_C=300.9 K) [13]. The spin wave stiffness data for the former show no evidence of the expected spin wave collapse at T_C, as in $La_{0.67}Ca_{0.33}MnO_3$ [14]. It is pointed out that the exotic spin dynamics in the low T_C manganite is related to the increased electron-lattice coupling [13].

Various theoretical models are proposed to explore the origin of the CMR phenomena. Among those, the combined model of the DE and the polaron explains the transport and other many experimental features rather well [15–17]. Indeed, this model could explain the resistivity and the magnetic behaviors of the high T_C manganites such as $La_{0.7}Ba_{0.3}MnO_3$. However, it appears that this model cannot describe a rapid drop of the resistivity below T_C and very large MR ratio of the low T_C manganites such as $La_{0.7}Ca_{0.3}MnO_3$. Including the effect of the phonon hardening below T_C improves the resistivity drop and the MR ratio substantially, but the characteristic magnetic field needed to reproduce the observed MR is still too high ($\sim 15 - 20$ T), as compared to the experimental value (~ 4 T) [18]. It is thus argued that the polaron model is not sufficient to explain the physics of CMR [19]. Therefore the central issue is whether the other mechanism than the the DE and the polaron should be invoked to understand the physics of CMR manganites.

Motivated by the very distinct behaviors in the resistivity and the magnetism between the low and high T_C manganites, we have reexamined the effects of the polaron transition in the combined model of the DE and the polaron. Employing the variational Lang-Firsov (VLF) canonical transformation, we have investigated the small-to-large polaron transition and explored its effects on magnetic and transport properties of both the low and high T_C manganites. Röder *et al.* [15] have tried a similar approach, but they did not show the transport properties explicitly in connection with the CMR phenomena. Millis *et al.* [16] have obtained comparable results using the dynamical mean field approximation, but the physics producing CMR is hidden and the resulting characteristic magnetic field needed to reproduce the observed MR is also too high.

In order to study the polaron transport incorporating the DE, we adopt the following Hamiltonian of the Zener-Holstein type:

$$\begin{aligned} H = -t\gamma(T) \sum_{i\delta} c^{\dagger}_{i+\delta} c_i + \sum_{\boldsymbol{q}} \omega_q a^{\dagger}_{\boldsymbol{q}} a_{\boldsymbol{q}} \\ + \sum_{i\boldsymbol{q}} c^{\dagger}_i c_i e^{i\boldsymbol{q}\cdot\boldsymbol{R}_i} M_q (a_{\boldsymbol{q}} + a^{\dagger}_{-\boldsymbol{q}}). \end{aligned} \tag{1}$$

Here the bandwidth variation by the DE is included in the hopping parameter with a factor $\gamma(T) = \langle \cos(\theta/2) \rangle$, where θ is the angle between local spins of neighboring Mn sites. M_q is the parameter representing the strength of the electron-phonon interaction. For simplicity but without loss of the physics, we consider the single e_g orbitals and the single phonon modes, which is plausible to describe the metallic phase of CMR manganites [15].

In the strong coupling ($E_p \equiv \sum_q M_q^2/\omega_q \gg t$) and the non-adiabatic limit ($\omega_q \gg t$), one can apply the conventional Lang-Firsov (LF) transformation and obtain the resistivity via the Kubo formula, considering the hopping term as a perturbation [17]. In the opposite weak coupling limit, the analytic solution can be obtained by treating the interaction term as a perturbation. It is, however, difficult to evaluate physical quantities in the intermediate regime inbetween.

We have adopted the VLF transformation to describe the small-to-large polaron transition and the associated physics in the intermediate regime. In the VLF method, one performs the Lang-Firsov transformation with some variational parameters and finds their values from the minimization conditions of the total energy. We follow the method of Das and Sil [20] in which three parameters are assumed: on-site lattice distortion Δ, nearest neighbor distortion Δ', and two-phonon coherent state parameter α. The coherent state allows for the anharmonicity of the lattice fluctuations, which become important at finite polaron densities and in the intermediate coupling and frequency regime [21]. The nearest neighbor distortion can be neglected in the three dimensional (3D) case for which the small-to-large polaron transition is so abrupt that Δ' does not contribute much in the course of the transition.

Using the VLF transformation, we have

$$\begin{aligned} \bar{H} &= e^{S} H e^{-S} \qquad\qquad (2) \\ &= -t\gamma(T) \sum_{j\delta} c^{\dagger}_{j+\delta} c_j X^{\dagger}_{j+\delta} X_j + \sum_{\boldsymbol{q}} \omega_q a^{\dagger}_{\boldsymbol{q}} a_{\boldsymbol{q}} \\ &\quad - E_p(2-\Delta)\Delta \sum_j n_j + (1-\Delta) \sum_{j\boldsymbol{q}} n_j M_q (a_{\boldsymbol{q}} + a^{\dagger}_{-\boldsymbol{q}}), \end{aligned}$$

with $S = -\sum_{j\boldsymbol{q}} \frac{M_q}{\omega_q} \Delta\, c^{\dagger}_j c_j e^{i\boldsymbol{q}\cdot\boldsymbol{R}_j} (a_{\boldsymbol{q}} - a^{\dagger}_{-\boldsymbol{q}})$, and $X_j = \exp\Big[\sum_{\boldsymbol{q}} \frac{M_q}{\omega_q} \Delta\, e^{i\boldsymbol{q}\cdot\boldsymbol{R}_j} (a_{\boldsymbol{q}} - a^{\dagger}_{-\boldsymbol{q}})\Big]$. Then, using the two-phonon coherent state $|\psi_{\rm ph}\rangle = e^{-\alpha \sum_{\boldsymbol{q}} (a_{\boldsymbol{q}} a_{-\boldsymbol{q}} - a^{\dagger}_{\boldsymbol{q}} a^{\dagger}_{-\boldsymbol{q}})} |0\rangle$ ($\alpha \geq 0$) as a trial phonon wave function, one can obtain the effective polaron Hamiltonian. Now the ground state energy is calculated in the framework of the mean-field theory:

$$\begin{aligned} \bar{E}/N = -2zt\gamma(T) \exp\left[-\frac{E_p}{\omega_0}\Gamma\right] n(1-n) + \omega_0 \sinh^2(2\alpha) \\ - nE_p(2-\Delta)\Delta, \end{aligned} \tag{3}$$

where $\Gamma \equiv \Delta^2 e^{-4\alpha}$, z is the coordination number, and $n = N^{-1} \sum_i n_i$ is the carrier density. We assumed a single phonon frequency ω_0. The values of Δ and α are obtained from the minimization of Eq. (3). With $\Delta = 1.0$ and $\alpha = 0$, that is, with $\Gamma = 1.0$, one can reproduce the result of the conventional LF transformation. Note that, in the VLF formalism, the effective hopping parameter is given by $\tilde{t} = t\gamma(T) \exp\Big(-\frac{E_p}{\omega_0}\Gamma\Big)$ with an additional parameter $\Gamma (\leq 1.0)$ in the polaron narrowing factor, so that the narrowing effect becomes weakened in the VLF formalism.

Figure 1 provides Γ and the polaron narrowing factor as a function of electron-phonon coupling constant $\lambda_p \equiv E_p/(2zt)$ for both the adiabatic and non-adiabatic cases. As shown in Fig. 1, the large-to-small polaron transition, the so-called self-trapping transition takes place near $\lambda_p \approx 1$ and is steeper for the adiabatic case. Also notable is that the critical value of λ_p^c at which the transition occurs is smaller for the adiabatic case. Though we do not show the results for 1D and 2D systems, the transition for 3D systems is steeper. These features are consistent with those obtained using other methods such as the exact diagonalization [22], the dynamical mean field approximation [23], and the quantum Monte-Carlo method [24,25]. Since the CMR manganites are close to 3D adiabatic systems, a very steep small-to-large polaron transition is expected.

It is tempting to interpret that the very steep self-trapping transition in Fig. 1 is the real first order phase transition. Caution is needed, however. According to the study of Löwen [26] for the Hamiltonian of the Holstein type, the self-trapping transition should be an analytical crossover not an abrupt (nonanalytical) phase transition. Indeed, numerical calculations for various model systems [22–25,27] show rather continuous self-trapping transitions. Then the seemingly nonanalytical transition seen in Fig. 1 may not be real but result from the shortcomings of the VLF method itself. Nevertheless, the general trend of the self-trapping transition obtained in Fig. 1 can be applied to CMR manganites for the analysis of transport and magnetic properties, by using a well-behaved function that smooth the nonanalytical transition (dots in the bottom panel of Fig. 1(a)).

To extend Eq. (3) to the finite temperature regime, the entropy term originating from the magnetic ordering must be included [28]. The resulting free energy per site is represented by

$$
\begin{aligned}
F = & -2zt\gamma(\nu)\,\exp\left[-\frac{E_p}{\omega_0}\Gamma(2N_0+1)\right]n(1-n) \\
& +\omega_0\left\{N_0\left[\sinh^2(2\alpha)+\cosh^2(2\alpha)\right]+\sinh^2(2\alpha)\right\} \\
& -nE_p(2-\Delta)\Delta - k_BT\left\{\ln[Q_S(\nu)]-\nu m_S(\nu)\right\}, \quad (4)
\end{aligned}
$$

where ν is the order parameter, $Q_S(\nu) = \sum_{M=-S}^{S}\exp(\nu M/S)$ is the partition function with spin $S = 2$, and $m_S(\nu)$ is the normalized magnetization per site. N_0 is the phonon distribution function and can be ignored in the temperature region of interest. $\gamma(T)$ is also a function of ν, being constant (0.6) for $T > T_C$ and increasing below T_C up to 0.8. Now the free energy is to be minimized instead of Eq. (3).

Upon cooling below T_C, the DE hopping parameter $t\gamma(T)$ increases. Accordingly, if λ_p decreases below λ_p^c, Γ becomes reduced a lot to weaken the polaron narrowing effect as seen in Fig. 1. This implies that Γ is an implicit function of the hopping parameter: with a larger hopping having reduced Γ. In consequence, the effective hopping parameter $\tilde{t}$ is rapidly enhanced to cause an enormous reduction of the resistivity below T_C (see Fig 3). In turn, this has an effect of increasing $\gamma(T)$ to make the magnetic transition much steeper than in the case of the DE only model. This feature will be discussed more in Fig. 2. The external magnetic field gives rise to the same effect, producing the CMR along with the bandwidth increment (Fig. 3).

From Eq. (4), T_C for $S = 2$ can be derived:

$$
k_BT_C = \frac{9}{50}\,2zn(1-n)\,t\exp\left[-\frac{E_p}{\omega_0}\Gamma\right]. \quad (5)
$$

This relation provides a possible account of the intriguing evolution of T_C with chemical pressure in $R_{0.7}A_{0.3}MnO_3$, determined by $\langle r_A\rangle$ [10]. This behavior is qualitatively understood in terms of the variation of the $\langle Mn-O\rangle$ bond length with $\langle r_A\rangle$ and the subsequent variation of the hopping parameter t [29]. However, the observed variation in the bond length, at most 1%, is thought to be too small to explain $\sim$ 500% variation in T_C. However, once employing the above polaron narrowing effects, one can account for the huge variation of T_C even with the small variation of the hopping parameter t. That is, the increase of $\langle r_A\rangle$ enhances t, and so reduces λ_p. As a result, Γ in the exponent of the polaron narrowing factor in Eq. (5) decreases so as to enhance T_C a lot. In a similar way, the decreasing isotope effect with $\langle r_A\rangle$ can also be understood by noting that the isotope exponent $\beta(\equiv -\Delta\ln T_C/\Delta\ln M_O$, M_O: oxygen isotope mass) is a decreasing function of the hopping parameter through Γ: $\beta \sim \frac{E_p}{\omega_0}\Gamma(t)$ [3].

Since we have determined the polaron narrowing factor for all the range of λ_p (Fig. 1), λ_{p0} for given T_C can be estimated using Eq. (5). We have larger λ_{p0} for lower T_C to have a higher slope of Γ at λ_{p0}, e.g., $\lambda_{p0} = 0.646$ and 0.619 for $T_C = 100$ K and 400 K, respectively, for parameters given in Fig. 2. Hence, as $\gamma(T)$ increases below T_C, the subsequent variation of λ_p drives a large reduction of Γ. Therefore one can expect a steeper magnetic transition and more rapid drop of the resistivity for low T_C manganites. Figure 2 presents the temperature dependent behaviors of the magnetization for various T_C. It is seen that the magnetic transition becomes steeper for lower T_C. Thus, the magnetic transition for $T_C < 200$ K is almost like the first order phase transition. Note, by contrast, that the magnetic transition in the DE only model takes place much more smoothly reflecting the second order phase transition. In view of these features, the change of magnetic properties in $La_{0.67}(Ba_xCa_{1-x})_{0.33}MnO_3$ with varying x can be elucidated [11]. Further, this feature provides a clue to describe the exotic spin dynamics observed in low T_C manganites. Since the transition is close to the first order phase transition, the coexistence between the paramagnetic and the ferromagnetic phase can occur in the course of the transition, manifesting features of the discontinuous drop of the hyperfine fields [12] and the spin wave stiffness [13] near T_c.

The routine evaluating the conductivity by means of the Kubo formula is the same as in Ref. [17] except for Γ in the polaron narrowing factor. Figure 3 shows the resulting resistivity as a function of temperature. Here the phonon hardening effect below T_C is also taken into account [18]. The M-I transition above T_C is clearly seen in the cases of low T_C. For $T_C = 100$ K, the resistivity peak is very sharp and the MR is very large. Note that the y-axis is in the log scale so that the resistivity drop below T_C amounts to three orders of magnitude. Hence the characteristic field for the observed MR becomes low enough, in agreement with the experiment. In the case of $T_C = 200$ K, we have $\sim$ 94% MR ratio for H = 5 T. In addition, the lower T_C manganites show higher resistivity in consistent with the experiments [10]. For higher T_C, the peak becomes dull, and eventually the M-I transition disappears for T_C larger than 300 K. This is again in agreement with the observation for $La_{0.7}Sr_{0.3}MnO_3$. One must note that the magnetic transition (Fig. 2) and the resistivity drop (Fig. 3) are steeper for low T_C manganites, demonstrating that both the CMR transport phenomena and the magnetic transition are closely correlated and are governed by the same physics.

Finally, it should be pointed out that the important effects, such as the double degeneracy of the e_g orbitals, the inter-orbital Coulomb correlation, and the Jahn-Teller effects, are not considered in the present study. One can in principle incorporating these effects, following the formalism by Zang *et al* [30]. The Jahn-Teller interaction yields the effective DE besides the Zener DE, and the Coulomb correlation gives rise to an additional band narrowing effect. Therefore, these effects are expected to enhance further the localization effect and the essential results of the present study will not be altered. The study that takes into account these effects explicitly is under progress.

In conclusion, we have investigated the small-to-large polaron crossover transition for the combined model of the polaron and the DE interaction and explored the effects of the polaron narrowing on the magnetic and transport properties of both the low and high T_C CMR manganites. We have shown that the polaron narrowing effect is much more pronounced in the low T_C manganites, which explains the rapid resistivity drop, large MR ratio, and the *first-order-like* sharp magnetic phase transition.

Acknowledgements− Helpful discussions with J.D. Lee are greatly appreciated. This work was supported by the KOSEF (96-0702-0101-3), and in part by the BSRI program of the KME (BSRI-98-2438).

---

[1] C. Zener, Phys. Rev. **82**, 403 (1951).
[2] P. W. Anderson and H. Hasegawa, Phys. Rev. **100**, 675 (1955).
[3] G. Zhao *et al.*, Nature **381**, 676 (1996).
[4] A. J. Millis *et al.*, Phys. Rev. Lett. **74**, 5144 (1995).
[5] S. J. L. Billinge *et al.*, Phys. Rev. Lett. **77**, 715 (1996).
[6] D. Louca *et al.*, Phys. Rev. B **56**, R8475 (1997).
[7] T. A. Tyson *et al.*, Phys. Rev. B **53**, 13985 (1996).
[8] C. H. Booth *et al.*, Phys. Rev. Lett. **80**, 853 (1998).
[9] A. Lanzara *et al.*, Phys. Rev. Lett. **81**, 878 (1998).
[10] H. Y. Hwang *et al.*, Phys. Rev. Lett. **75**, 914 (1995).
[11] N. Moutis *et al.*, Phys. Rev. B **59**, 1129 (1999).
[12] M. M. Savosta *et al.*, Phys. Rev. Lett. **79**, 4278 (1997).
[13] J. A. Fernandez-Baca *et al.*, Phys. Rev. Lett. **80**, 4012 (1998).
[14] J. W. Lynn *et al.*, Phys. Rev. Lett. **76**, 4046 (1996).
[15] H. Röder *et al.*, Phys. Rev. Lett. **76** 1356 (1996).
[16] A. J. Millis *et al.*, Phys. Rev. Lett. **77**, 175 (1996).
[17] J. D. Lee and B. I. Min, Phys. Rev. B **55**, 12454 (1997).
[18] U. Yu, J. D. Lee, and B. I. Min (unpublished).
[19] A. S. Alexandrov and A. M. Bratkovsky, Phys. Rev. Lett. **82** 141 (1999).
[20] A. N. Das and S. Sil, J. Phys.: Condens. Matter **5**, 8265 (1993).
[21] H. Zheng, Solid State Comm. **65**, 731 (1988).
[22] M. Capone, W. Stephan, and M. Grilli, Phys. Rev. B **56**, 4484 (1997).
[23] S. Ciuchi *et al.*, Phys. Rev. B **56**, 4494 (1997).
[24] H. de Raedt and A. Lagendijk, Phys. Rev. B **27**, 6097 (1983).
[25] P. E. Kornilovitch, Phys. Rev. Lett. **81**, 5382 (1998).
[26] H. Löwen, Phys. Rev. B **37**, 8661 (1988).
[27] H. Fehske *et al.*, Phys. Rev. B **51**, 16582 (1995).
[28] K. Kubo and N. Ohata, J. Phys. Soc. Jpn. **33**, 21 (1972).
[29] P. G. Radaelli *et al.*, Phys. Rev. B **56**, 8265 (1997).
[30] J. Zang *et al.*, Phys. Rev. B **53** 8840 (1996).

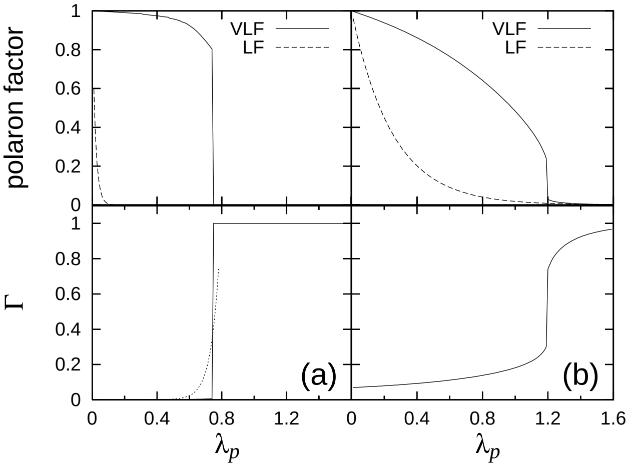

FIG. 1. The polaron narrowing factor $\exp\left[-\frac{E_p}{\omega_0}\Gamma\right]$ and the parameter Γ as a function of λ_p for the 3D systems with $n = 0.3$ obtained using the VLF transformation: (a) the adiabatic case ($\omega_0/t = 0.13$) and (b) the non-adiabatic case ($\omega_0/t = 3.0$). Results of the conventional Lang-Firsov (LF) transformation ($\Gamma = 1.0$) are also presented in the top panel for comparison. Dots in the bottom panel of (a) represent an illustration of the continuous well-behaved function smoothing the abrupt self-trapping transition.

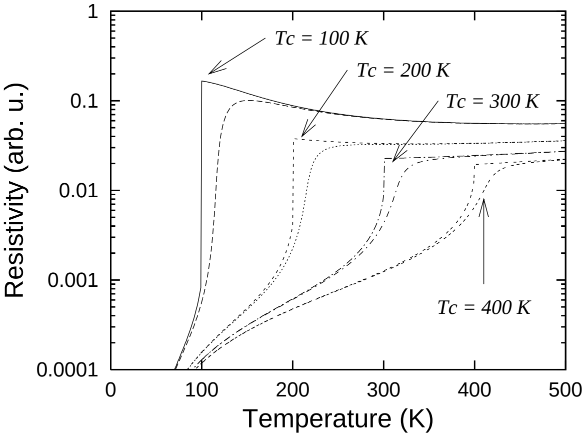

FIG. 2. Magnetization vs. temperature for various T_C's. Result in the DE only model is also presented for comparison. Parameters used in the calculation are $t\gamma(T_C) = 0.3$ eV and $\omega_0 = 0.04$ eV.

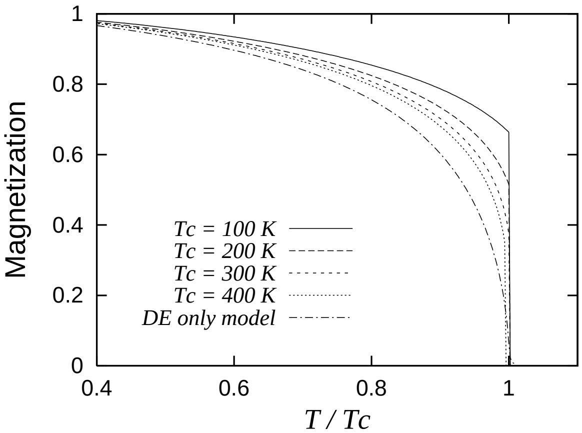

FIG. 3. Temperature dependent resistivity without and with the magnetic field of 5 T (lower curves) for various T_C's. Note that the y-axis is in the log scale. Parameters used in the calculations are the same as in Fig. 2.